Pitx2-Mediated Cardiac Outflow Tract Remodeling

Hsiao-Yen Ma[1], **Jun Xu**[1], **Diana Eng**[1], **Michael K. Gross**[1], and **Chrissa Kioussi**[1,*]

[1]Department of Pharmaceutical Sciences, College of Pharmacy, Oregon State University, Corvallis, OR 97331, USA

Abstract

Background—Heart morphogenesis involves sequential anatomical changes from a linear tube of a single channel peristaltic pump to a four-chamber structure with two channels controlled by one-way valves. The developing heart undergoes continuous remodeling, including septation.

Results—Pitx2-null mice are characterized by cardiac septational defects of the atria, ventricles, and outflow tract. Pitx2-null mice also exhibited a short outflow tract, including unseptated conus and deformed endocardial cushions. Cushions were characterized with a jelly-like structure, rather than the distinct membrane-looking leaflets, indicating that endothelial mesenchymal transition was impaired in Pitx2$^{-/-}$ embryos. Mesoderm cells from the branchial arches and neural crest cells from the otic region contribute to the development of the endocardial cushions, and both were reduced in number. Members of the Fgf and Bmp families exhibited altered expression levels in the mutants.

Conclusion—We suggest that Pitx2 is involved in the cardiac outflow tract septation by promoting and/or maintaining the number and the remodeling process of the mesoderm progenitor cells. Pitx2 influences the expression of transcription factors and signaling molecules involved in the differentiation of the cushion mesenchyme during heart development.

Keywords

heart; development; cardiac outflow tract; homeobox; Pitx2

INTRODUCTION

Congenital heart defects are the leading non-infectious cause of death in newborns. Approximately half of all cases are associated with septational malformations in the outflow tract (OT) and/or ventricles (Hoffman and Kaplan, 2002). The mammalian heart develops from cells of four embryonic origins: (1) the cardiac crescent, first lineage or first heart field; (2) the branchial arch (BA)-derived mesoderm, second lineage or secondary heart field; (3) the cardiac neural crest (cNC) cells and (4) the epicardium. The first lineage appears shortly after gastrulation as a population of mesodermal cells that differentiate into endocardial and myocardial types and form a tubular structure (Harvey, 2002). The second lineage arises from a population of splanchnic mesodermal cells that contribute to the formation of OT and right ventricle (RV) (Kelly et al., 2001; Buckingham et al., 2005). The OT is a tubular structure consisting of striated cardiac musculature lined with endocardium. The OT follows a dramatic remodeling to form the aorto-pulmonary (AP) septum that separates the initially single OT vessel to form the ascending aorta (Ao) and the pulmonary trunk (Webb et al., 2003). Between E9.5 and E10.5, endocardial cushions start to form across the common OT, the conotruncus, and the atrioventricular canal. The conotruncal

*Correspondence to:chrissa.kioussi@oregonstate.edu, T 541-737-2179, F 541-737-3999.

endocardial cushions further divide into proximal and distal conotruncal cushions. The distal conotruncal cushions will form the AP septum at E12.5 – E13.5. The linear heart tube consists of the external layer of myocardium and the internal layer of endocardium, which are separated by the myocardium-produced extracellular matrix, the cardiac jelly. As endocardial cushions develop, endocardial cells proliferate and undergo an epithelial-to-mesenchymal transformation (EMT) and infiltrate the cardiac jelly. As the two cushions come closer, the endocardial cell barrier degenerates and the mesenchymal cells form a bridge to stabilize the fusion of the two cushions (Ray and Niswander, 2012). When tissue alignment, fusion or rotation is disrupted, transposition of the great arteries (TGA) or double-outlet right ventricle (DORV) occurs. Complete failure of OT septation results in persistent truncus arteriosus (PTA).

At the early stages, cNC cells penetrate the second lineage, which is adjacent to the pharyngeal ectoderm, for the formation of the OT. The unspecified mesoderm receives extracellular cues that orchestrate its sequential differentiation into cardiogenic mesoderm, myocardium and smooth muscle. These cues are primarily signaling molecules, such as the bone morphogenetic proteins (BMPs) and the fibroblast growth factors (FGFs). BMP signaling is involved in the induction of the cardiac differentiation. Bmp2 and Bmp4 induce Nkx2.5 and Gata4, which regulate differentiation of cardiac mesoderm into first and second heart lineages (Monzen et al., 1999). *BMP* signaling promotes specification and differentiation of the second lineage to a cardiac fate by inhibiting FGF signaling (Tirosh-Finkel et al., 2006). *Bmp4* is expressed in the splachnic mesoderm, BA mesoderm, and OT myocardium, and is required for OT septation and endocardial cushion remodeling (Liu et al., 2004). FGF signaling is involved in cardiac induction, septation, cell proliferation and OT alignment (Kelly et al., 2001; Ilagan et al., 2006; Park et al., 2008).

Sequence-specific transcription factors (SSTFs) are also involved in guiding proper cardiac cellular proliferation, differentiation and migration. The LIM-homeodomain protein Islet-1 (Isl1) is expressed in the pharyngeal mesoderm and is required for the development of the SHF lineage and its derivatives (Cai et al., 2003). Isl1 marks proliferating, undifferentiated pluripotent cardiovascular progenitors of the second lineage (Cai et al., 2003; Buckingham et al., 2005). *Isl1*-null mice die at E10 with hearts lacking OT septation. The bHLH protein Mef2c marks a subpopulation of the second lineage (Dodou et al., 2004) and, when mutated, leads to similar defects as *Isl1*, including defective heart looping and malformed OT (Lin et al., 1997; Buckingham et al., 2005). *Tbx1* is expressed in the non-cNC-derived mesoderm of the caudal pharyngeal region, which is part of the second lineage and contributes to the formation of OT and RV (Hu et al., 2004; Xu et al., 2004). *Fgf8* and *Fgf10* act downstream of Tbx1 in the second lineage (Vitelli et al., 2002; Kelly and Papaioannou, 2007).

Pitx2, a paired-like homeobox SSTF, is transiently expressed on the left side of the cardiac crescent and linear heart tube during early development (E8), and later (E9–E14.5) is expressed in the OT and RV. Genomic screens for inherited atrial fibrillation patients have found deficiencies in the Pitx2 locus (Schnabel, 2011). Pitx2-null embryos are characterized by a non-septated atrium, valvular and OT deficiencies, including PTA, DORV and TGA (Gage et al., 1999; Kitamura et al., 1999; Lin et al., 1999; Lu et al., 1999; Kioussi et al., 2002). Pitx2 controls the specification of cardiac cells within the second lineage by repressing Fgf10 and Isl1 (Galli et al., 2008). Pitx2 and Tbx1 are necessary for proper migration and proliferation of secondary lineage cardiac progenitors (Nowotschin et al., 2006). The observed phenotypes of the knockout mouse models indicated that Pitx2 is critical in regulating the OT formation. Here we report that Pitx2 acts in a network kernel during cardiogenesis and controls the state of the cells of the second lineage as they migrate from the BA to OT and enter the remodeling state to form the valves.

RESULTS

Hypocellular OT Endothelial Cushions in Pitx2 Mutants

Pitx2-null mice (*Pitx2^LacZ/LacZ^*, *Pitx2^Z/Z^*) die at E14.5 due to arrest of organ development (Gage et al., 1999; Kitamura et al., 1999; Lin et al., 1999; Lu et al., 1999). The heart is one of the organs that is severely affected, displaying atrial and ventricular septal defects, hypoplastic RV, RA isomerism, DORV, TGA, PTA and abnormal aortic arch remodeling (Gage et al., 1999; Kitamura et al., 1999; Lin et al., 1999; Lu et al., 1999; Campione et al., 2001; Liu et al., 2002). The phenotype of the developing OT was analyzed at E10.5 and E12.5 in mutant and wild type mice (Fig. 1). At E10.5, the heart was already smaller, with delayed looping (Fig. 1A, B). The length of the OT was measured in at least three groups of mice, and a 20% decrease was identified (Fig. 1C), as has been also previously described (Ai et al., 2006). As the heart matures, it undergoes remodeling, and at E12.5 the OT divides and forms two structures, the aorta (Ao) and pulmonary artery (PA) (Fig. 1E). The septation of the OT occurs by (1) the initial division of the aortic sac by the cNC cells, (2) the septation of the distal part of the OT (truncus), and (3) the zipper-like closure of the proximal part (conus) through the fusion of the cushions (Kirby, 2007). By E12.5, septation of the truncus, including the semilunar OT valves, has been completed. The conus closes from distal to proximal towards the ventricles. The ridges beneath the endocardium start to bulge, and when they meet in the middle of the lumen, the endocardium breaks down and a septum is formed (Waldo et al., 1998; Waldo et al., 1999). This conal septum separates the pulmonary and aortic roots. The Pitx2 mutants that exhibited DORV (Fig. 1F) continued to exhibit a shorter OT by 20% (Fig. 1G). Histological analysis on transverse sections at the conus level (Fig. 1E1, F1) indicated a thin and loose epithelium, a non-septated conus with randomly arranged mesenchymal cells within the semilunar valves, in the mutants (Fig. 1F1). Cell-counts of serial transverse sections through the OT of three individual mice for each stage indicated a slow but consistent cell reduction during OT valve formation, starting with no significant reduction at E10.5 (Fig. 1D) followed by a 17.5% reduction at E12.5 (Fig. 1H). Double labeling immunohistochemistry for MF20 and Pitx2(β-Gal) on transverse sections at the level of the pulmonary and aortic roots at E12.5 (Fig. 1I, J) indicated lack of MF20^+ cells between the roots in mutants (Fig. 1J). Pitx2 was expressed in the muscularized semilunar pulmonary and aortic valves (Fig. 1I, yellow cells). No MF20^+ cells were detected in these cells in mutants (Fig. 1J). These data collectively suggest that Pitx2 is involved in the formation of the OT septum and in the muscularization process of the pulmonary and aortic valves.

Cell Death and Proliferation Defects of OT Mesenchymal Cells in *Pitx2* Mutants

During cardiac remodeling, the OT cushions undergo EMT and become the membranous valves upon activation of cell apoptosis. To determine if Pitx2 is involved in this mechanism, Pitx2-mutant and heterozygote littermates were examined for TUNEL and BrdU incorporation (Fig. 2). No cell death differences were detected at E10.5 (Fig. 2A, B). By E12.5, the OT undergoes remodeling and mesenchymal cells follow programmed cell death (Fig. 2C, arrows). No such cells were detected in the mutants (Fig. 2D). Cell-counts of OT serial sections at E12.5 showed significant decrease of TUNEL^+ cells in the mutants (Fig. 2E). To assay for cell proliferation, BrdU^+ and BrdU^+/Pitx2^+(β-Gal^+) mesenchymal cells were detected by double labeling immunohistochemistry at E10.5 (Fig. 2F, G) and E12.5 (Fig. 2I, J). Cells were counted in five serial sections from three independent embryos at each stage and genotype. The number of BrdU^+ cells was 20% higher in mutants at both stages, while the number of BrdU^+/Pitx2^+ cells was increased by 57% at E10.5 and 65% at E12.5 (Fig. 2H, K). Collectively these data suggest that Pitx2 maintains the number of mesenchymal cells by inhibiting them from entering the cell cycle and promoting their exit, for further differentiation and/or apoptotic fate.

Second Cell Lineage and cNC Cell Defects in *Pitx2* Mutants

Expression of Pitx2 in the OT cushions is detected as early as E10, and absence of Pitx2 results in a non-septated aorta and pulmonary trunk (Gage et al., 1999; Kitamura et al., 1999; Lin et al., 1999; Kioussi et al., 2002). To investigate the cellular events, the Mef2c-lineage tracer mouse was crossed to $Rosa^{EGFP}$ to detect the second cell lineage (Verzi et al., 2005). Double labeling immunohistochemistry was used to determine the distribution of EGFP(Mef2c) and Isl1 in BAs (Fig. 3A, B) and OT (Fig. 3D, E) at E10.5. Mef2c is restricted to the second lineage, while Isl1 primarily marks the cardiac progenitor cells (Cai et al., 2003) and, to a lesser extent, the cNC cells (Engleka et al., 2012). EGFP[+]/Isl1^{+} cells were detected as they enter the heart tube (Fig. 3A) and were severely reduced in the mutants (Fig. 3B). The EGFP^{+} cells were also already very much reduced in the BAs (Fig. 3B). The EGFP[+]/Isl1^{+} cells located in several layers of the OT epithelium (Fig. 3D) were reduced in mutants (Fig. 3E). The EGFP^{+} cells that contribute to the formation of the epithelium and leaflets (Fig. 3D) were also reduced in the mutants (Fig. 3E). These cellular defects were more prominent at E12.5 (Fig. 3G, H). Very few EGFP[+] and almost no Isl1^{+} cells were detected in the OT epithelium and leaflets. Quantitative assays indicated almost 50% reduction of EGFP(Mef2c) in BA (Fig. 3C) and the entire heart (Fig. 3F, I) compared to wild type embryos. Isl1 RNA levels were also reduced in the tested biopsies but in less extent (Fig. 3C, F, I). RNA levels for both EGFP and Mef2c were measured and no difference was detected in both BA and OT, suggesting that EGFP levels correspond to the endogenous Mef2c.

The cNC cells also contribute to the OT endocardial cushions. Postotic NC cells contribute to OT endocardial cushions (Kirby, 2007); preotic NC cells distribute to the contruncus and coronary artery formation (Arima et al., 2012). To test the cNC distribution in the OT of the Pitx2 mutants, the $Wnt1^{Cre}/Rosa^{EGFP}$ reporter mouse was crossed to the $Pitx2^{LacZ}$ line. Although the contribution of the Wnt1^{+} cells to the OT under the Pitx2 influence was previously reported, (Ai et al., 2006), we performed the analysis at earlier developmental stages. At E9.5 the OT is already shorter in the Pitx2 mutants, (Fig. 4B) and the Wnt1^{+} cells just populated the OT; while in the control wild type mice, they start to fuse and widely populate the area (Fig. 4A). At E10.5, a thick stream of Wnt1^{+} cells was located in the OT (Fig. 4C); while in the mutants, this population seems restricted to the truncated truncus (Fig. 4D). At E12.5 this delay of the Wnt1^{+} cells to populate the truncus and conus seems to be recovered in the mutants (Fig. 4E, F). However, the expression levels of another cNC marker, Ap2α, were reduced in the OT in mutants (Fig. 4G, H) at E12.5. These data suggest that Pitx2 influences the distribution of the BA mesoderm derived and cNC cells during OT and endocardial cushion development.

Pitx2 Occupancy at SSTF Loci in BAs and Heart

Our data have shown that Pitx2 regulates the expression of both Mef2c and Isl1 in the BAs and OT, indicating this regulation might be on a transcriptional level. Chromatin-occupancy analyses provided another means to assess the interaction between Pitx2 and the SSTF that were altered in E10.5 *Pitx2* mutants. Embryos from approximately 2–3 synchronous litters were rapidly genotyped. Tissue biopsies, including BA (mandibular part of 1st, 2nd and 3rd BA) and heart (OT, atria and ventricles), were dissected from 6–8 embryos of each genotype and pooled for two independent experiments. From each experiment, a pair of wild type and mutant chromatin extract was generated with sufficient material for one immunoprecipitation, using an anti-Pitx2 antibody. Each immunoprecipitate provided enough material for 15 triplicate qPCR analyses. Amplicons within the *Mef2c, Isl1, Gat4* and *Nkx2.5* loci were identified, as described previously for T-box (Hilton et al., 2010) and Hox (Eng et al., 2012) genes. Core motifs for bicoid class homeodomains (TAATCY) that were embedded in evolutionarily conserved non-coding regions and were, themselves,

evolutionarily conserved, were identified (Fig. 5). Each red diamond represents a different species in which the core motif was conserved and expected to be essential for biological function. Core motifs with the most diamonds were selected as candidate *cis* regulatory modules, and primer pairs were designed to encompass a 70–150 bp context around these sites. The initially selected primer pairs were tested by endpoint PCR on purified genomic DNA. Amplified pairs were selected for SSTF chromatin occupancy analyses by ChIP-qPCR (Table 1). The mutant extract lacks Pitx2 protein and is, therefore, expected to have 0% occupancy. The signal measured in the mutant precipitate, for any given amplicon, is a direct measurement of the background. Pitx2 occupied *Mef2c* (Fig. 5A, B) and *Isl1* (Fig. 5C, D) in the BA biopsies at positions −521 and +1983, respectively. No Pitx2 occupancy was detected on *Gata4* (Fig. 5F) at the positions −1065, +29818 and +36199, despite being evolutionarily conserved (Fig. 5E). Pitx2 occupancy was also not detected on *Nkx2.5* (Fig. 5H) at the positions −10523 and −1952 (Fig. 5G). Pitx2 occupancy on *Tbx1* BA biopsies has previously been reported in E10.5 mice (Shih et al., 2007a). The Pitx2 occupancy on the SSTF *Mef2c* and *Isl1* correlates well with their altered expression profiles in the developing BA. It has been shown that Pitx2 regulates *Gata4* expression (Lozano-Velasco et al., 2011), and *Nkx2.5* has synergistic activity with Pitx2 (Ganga et al., 2003). However, this might not be due to Pitx2 occupancy at this developmental stage.

Pitx2 and FGF/BMP Signaling

FGF signaling in the second cardiac lineage is essential for OT cushion formation and remodeling. *Fgf8* expression in the ectoderm of the 1st and 2nd BA regulates proliferation and differentiation of post-migratory cNC cells. FGF signaling in the OT myocardium controls extracellular matrix formation; while BMP signaling is essential for endothelial cell transformation and invasion of cNC cells (Park et al., 2008). RNA in situ hybridization at E10.5 was used to determine the expression profile of *Fgf8, Fgf3, Bmp4* and *Notch* (Fig. 6). *Fgf8* is detected in the ectoderm of the 2nd, 3rd and 4th BA in wild type and heterozygote embryos (Fig. 6A, B) and was barely detectable in the 4th BA in mutants (Fig. 6C), as previously described (Liu et al., 2003). Similarly, the area of *Fgf3* expression in the 3rd – 6th BA (Fig. 6E, F) was reduced in mutants (Fig. 6G). The *Notch* signaling has been implicated in regulating EMT during valve development. *Notch2* is expressed in the cNC-derived vascular smooth muscle cells and is critical in mammalian OT development (Niessen and Karsan, 2008). *Notch2* was expressed in the 3rd and 4th aortic arch (Fig. 6I, J), with significantly reduced expression levels in the mutants (Fig. 6K). *Bmp4* is expressed in the ventral splanchnic mesoderm, BA mesoderm, and OT myocardium. Bmp4 promotes proliferation of cushion mesenchyme and concurrently represses cell proliferation in the OT myocardium (Liu et al., 2004). The *Bmp4*-distinct area of mesenchymal expression in the OT (Fig. 6M, N) was not detected in mutants (Fig. 6O). The thinner OT epithelium was prominent in all mutants (Fig. 5M, N, O, red and black dotted line). Quantitative PCR analysis further confirmed the lower expression levels of *Fgf8* (Fig. 6D), *Fgf3* (Fig. 6H), *Notch2* (Fig. 6L) and *Bmp4* (Fig. 6P) in the mutant BA and heart (only for *Bmp4*) biopsies at E10.5. No significant difference between wild type and heterozygote was detected. Collectively, these results suggest that the combination of the altered *FGF*, *BMP* and *Notch* signaling results in the hypoproliferative mesenchymal cells in the OT cushions and their delayed EMT.

Cardiac Vascular and Innervation Defects in *Pitx2* Mutants

Unilateral ablation of *Pitx2* results in asymmetric remodeling of the BA system, which leads to randomized laterality of the aortic arch (Yashiro et al., 2007). We investigated the aortic arch system defects, found in the Pitx2 mutants at the cellular level, by whole mount antibody staining with platelet-endothelial cell adhesion molecule (PECAM) at E10.5 (Fig. 7A, B, D, E). Endothelial cells were detected in the well-developed 3rd and 4th BAs and, to a

lesser extent, in the 6th BA (Fig. 7A). An increased number of endothelial cells were extending into the OT and RV in wild type mice (Fig. 7A, D). In contrast, endothelial cells were severely reduced in mutant BAs (Fig. 7B) and OT (Fig. 7E). A similar phenotype was also observed at E11.5 (data not shown). Quantitative PCR further confirmed the reduced PECAM level of expression in mutant BA (Fig. 7C) and heart biopsies (Fig. 7F). The BA innervation process was also affected in Pitx2-null mutant mice as detected by whole mount neurofilament (NF) antibody staining (Fig. 7G, H, J, K). The maxillary (V2) (Fig. 7G, H, red dotted line) and mandibular (V3) (Fig. 7G, H, star) branch of the trigeminal nerve (V) that innervates mastication muscles was not prominent in the mutants. Pitx2 mutants do not form mastication muscles (Shih et al., 2007a); and, thus, V2 and V3 were unable to migrate to their final destinations, as the supportive tissue was missing. The facial nerve (VII) that innervates the facial muscles and receives the sense from the anterior tongue was distorted. It failed to reach the edge of the 2nd BA (Fig. 7G, H). The sensory acoustic nerve (VIII) that migrates parallel to VII had a similar phenotype (Fig. 7G, H). The glossopharyngeal nerve (IX) provides special innervation to the stylopharyngeus. The vagus nerve (X) provides brachiomotor innervation to the majority of laryngeal and pharyngeal muscles and has three nuclei associated with the cardiovascular control the dorsal motor nucleus, the nucleus ambiguous, and the solitary nucleus. The afferent fibers of the autonomic nervous system transmit signals to the medulla by cranial nerves X and IX. Both IX and X nerves, located in the jugular area, were thinner, shorter, and not properly aligned in mutants, possibly as a result of the severe distortion or absence of several facial muscles (Fig. 7G, H). The X nerve innervates the OT to sense the aortic blood pressure and to slow the heart rate (Fig. 7G, arrow). NF expression was detected in the wild type (Fig. 7J) heart but in much lower levels than in mutants (Fig. 7K). This signal reduction may explain the observed arrhythmias and conduction deficiencies in Pitx2-mutant mice and human patients (Schnabel, 2011). Quantitative analyses for NF (Fig. 7I, L) were also performed in BAs (Fig. 7I) and heart (Fig. 7L) biopsies, indicating significant reduction of NF in mutants.

DISCUSSION

Homeobox genes are key players for cell specification and organ formation as members of network kernels at early developmental stages. Pitx2 specifies tooth, pituitary, (Gage et al., 1999; Kitamura et al., 1999; Lin et al., 1999; Lu et al., 1999; Shih et al., 2007b), facial (ocular and mastication) (Gage et al., 2005; Shih et al., 2007a) and abdominal (Hilton et al., 2010) muscle development, while regulating the developmental process of organs including heart, intestine and lung (Gage et al., 1999; Kitamura et al., 1999; Lin et al., 1999; Lu et al., 1999; Shih et al., 2007b). The human Axenfeld-Rieger syndrome associated with mutations in *PITX2* locus 4q25 is characterized by umbilical hernia, glaucoma, myopathies and cardiac arrhythmias (Perveen et al., 2000; Schnabel, 2011). The close correlation of mouse phenotypes to the human syndrome demonstrates the evolutionarily conserved functions of Pitx2. Pitx2 loss of function results in severe cardiovascular defects, including atrial isomerism, DORV, TGA, PTA and abnormal aortic arch remodeling (Gage et al., 1999; Kitamura et al., 1999; Lin et al., 1999; Lu et al., 1999; Campione et al., 2001; Liu et al., 2002). Genetic studies have shown that Pitx2-mediated signaling during cardiogenesis is conducted within BA mesoderm cells (Ai et al., 2006), pharyngeal arch mesenchyme (Franco and Campione, 2003) and cNC cells (Hamblet et al., 2002; Kioussi et al., 2002). Our data show that *Pitx2* is a member of a network kernel, including *Mef2c*, *Isl1*, *Tbx1*, *Gata4* and *Nkx2.5*, that synergistically regulates endocardial cushion development and separation of the great arteries. We have demonstrated that Pitx2 occupies *cis* regulatory elements of *Mef2c*, *Isl1* and *Tbx1* (Harel I, 2012) in BA mesoderm.

Conotruncal defects, including TGA, DORV, tetralogy of Fallot, and PTA, result in abnormal OT development, including hypocellular cushions, altered conotruncal rotation,

and misalignment of septal components. Endocardial cushion formation starts with a swelling of the OT region at E9.5 and their formation is induced by signals from the myocardium that inhibit expression of chamber-specific genes and the active expression of extracellular matrix genes. BMPs are the major myocardial signals that initiate endocardial cushion formation and remodeling by promoting EMT (Lyons et al., 1990; Ma et al., 2005). Bmp4 is required for endocardial cushion expansion and OT septation (McCulley et al., 2008). Loss of Bmp4 in the second cardiac lineage results in a limited number of cells in the developing OT cushions and a defective remodeling process, a very similar phenotype to the one observed in the *Pitx2*-mutant mice. BMP signaling in the endocardium and cNC cells is vital to OT septation and formation of the aorta and pulmonary arteries.

TGFβs are among the early signaling molecules implicated in endocardial cushion development. TGFβ ligands and receptors are expressed in the OT during cushion formation and EMT (Brown et al., 1996). TGFβ signaling acts through SMADs to induce expression of the SSTF Slug that, in turn, promotes endocardial cushion formation of the antrioventricular canal (AVC) via EMT mechanisms (Romano and Runyan, 2000). Wnt/β-catenin regulates cardiac valve formation (Hurlstone et al., 2003) and, together with TGFβ, regulates cushion EMT. Notch signaling induces the expression of the pro-migratory SSTF Snail in AVC and OT endocardial cushion endothelial cells undergoing EMT. Snail inhibits VE-cadherin activity, and mesenchymal cells break contact with their neighboring cells. Notch signaling is also required for TGFβ2 and several TGFβ receptors in AVC and OT to further support endocardial EMT.

Fgf10, a target of the Wnt-β-catenin pathway in the cardiac mesoderm, is expressed in the second cardiac lineage (Kelly et al., 2001). However, Fgf10-null mice do not exhibit apparent cardiac defects. Fgf8 is also expressed in the second cardiac lineage and, when mutated, results to DORV and PTA (Abu-Issa et al., 2002; Frank et al., 2002). Fgf8 is essential for mesoderm-derived cell proliferation and survival during OT elongation. Reduced expression of Fgf8 in mesoderm- and ectoderm-derived cells, resulting in apoptotic cNC cell death in the developing pharyngeal arches (Ilagan et al., 2006).

Cardiac NC cells migrate into the OT endocardial cushions and contribute to the formation of aortic and pulmonary valves. Ablation of cNC cells results in OF defects, including shortening in length, delayed rotation and caudal displacement, dextroposed aorta (DORV), PTA, and interruption of the aortic arch. The shorter OT is also characterized by decreased second cardiac lineage cell migration (Waldo et al., 2005). This reciprocal interaction between the two cell lineages is essential for the OT septation.

Pitx2 acts upstream of the Wnt11/TGFβ2 signaling pathway that regulates extracellular matrix composition, cytoskeletal rearrangements and polarized cell movement required for tissue morphogenesis (Zhou et al., 2007). *BMP* and *Notch* expression was Pitx2-dependet in the OT of the linear heart tube in areas where cushions will be formed (Fig. 6I–K, M–O). This further supports the involvement of Pitx2 in a multi-signaling network during cushion formation and EMT induction and maintenance. *Pitx2*-mutant mice also exhibit remodeling malformations of intraventricular septum and ventricular myocardium (Tessari et al., 2008). The formation of AVC and the ventricular septation is another type of cell fusion that requires EMT.

Thus, we conclude that Pitx2 regulates the maintenance and epithelial-mesenchymal transitions of the BA mesoderm cells as they enter the linear heart tube to form the OT endocardial cushions. Pitx2 promotes the healthy interaction of the mesoderm-derived and cNC cells for proper OT septation by acting as a node of a sophisticated network kernel.

EXPERIMENTAL PROCEDURES

Mice

ICR $Pitx2^{+/LacZ}$ ($Pitx2^{+/Z}$) mice (Lin et al., 1999) were bred and females were checked for the presence of a vaginal plug (E0). Embryos were isolated at different developmental stages and the yolk sacs were used for genotyping. $Mef2c^{Cre}$ mice (Verzi et al., 2005) and $Wnt1^{Cre}$ mice (Jackson Lab) (Echelard et al., 1994) were crossed with $Rosa26^{EGFP}$($Rosa^{EGFP}$) (Jackson Lab) (Mao et al., 2001) mice to obtain $Mef2c^{Cre}|Rosa^{EGFP}$ and $Wnt1^{Cre}|Rosa^{EGFP}$ double heterozygotes, respectively. $Pitx2^{+/Z}$ mice were crossed with $Mef2c^{Cre}|Rosa^{EGFP}$ or $Wnt1^{Cre}|Rosa^{EGFP}$ to generate green $Pitx2$ wild type and mutant mice. PCR analysis from tail genomic DNA identified the 380 bp EGFP and 400 bp Cre bands.

Immunohistochemistry, TUNEL and BrdU

Immunohistochemistry on cryosections was performed as described by (Shih, 2007). Sections were photographed on an AxioImager Z1, Zeiss microscope. TUNEL assay was also performed as recommended by the manufacturer (Dead End kit; Promega). Pregnant female $Pitx2^{+/Z}$ mice were injected with 5 mg/ml BrdU 2 hr before dissection. Embryos from injected mice were processed, as previously described (Shih et al., 2007a). Immunohistochemistry of whole-mount embryos was performed according to standard protocol (Joyner and Wall, 2008). Whole embryos were photographed with a discovery V8, Zeiss microscope. Primary antibodies are listed as follows: MF20 (Mouse, 1:50, DHSB), β-galactosidase (Rabbit, 1:1000, Cappel), BrdU (Rat, 1:100, Accurate Chemical Scientific Corporation), EGFP [Rat, 1:1500, (Shih et al., 2007b)], Isl1 (Mouse, 1:30, DHSB), PECAM (Rat, 1:10, BD Biosciences), Neurofilament 200 (Rabbit, 1:100, Sigma).

Quantitative Real-time PCR(qPCR)

cDNA from BA (n=5) and heart (n=5) were prepared by RNeasy Micro Kit (Qiagen). cDNA (25ng) was analyzed by qPCR using SYBR Green I methodology as previously described (Hilton et al., 2010). All samples were analyzed in triplicate and normalized by glyceraldehyde-3-phosphate dehydrogenase. All qPCR primer sets are listed in Table 1.

Pitx2-Binding Site Analysis

An in house Perl script, binding_site_compare.pl was used for identifying the absolute location and evolutionary conservation of potential Pitx2-binding sites TAATCY (Amendt et al., 1998; Eng et al., 2010; Campbell et al., 2012; Eng and Dubovoy, 2012). The alignments for each gene, along with the 20kb region upstream of the gene, were download from the UCSC Genome Browser on Mouse July 2007 (NCBI37/mm9) Assembly, available at http://genome.ucsc.edu/. The alignments were then formatted for our script, which identified the absolute location of potential Pitx2 binding sites and the species conserved for each binding site. Excel was used to map binding site locations and species to each gene.

Chromatin Immuno-Precipitation (ChIP)

Heart and BA biopsies from 6–8 embryos of E10.5 $Pitx2$ wild type and $Pitx2^{Z/Z}$ mice were harvested per ChIP. Samples were collected and processed as previously described (Hilton et al., 2010). Primers were designed for binding sites identified as conserved sites. Control primers were designed for regions on the genome with no putative binding site within a minimum of a 1kb window on the mouse genome. All primer sets are listed in Table 1.

RNA in situ Hybridization

Whole-mount RNA in situ hybridization was performed according to standard procedures (Oliver et al., 1995). RNA in situ hybridization on sections was performed on 16 μm

cryosections, as previously described (Kyrylkova et al., 2012). Digoxigenin-labeled antisense RNA in situ probes were generated by an in vitro transcription kit (Dig RNA labeling kit, Roche Molecular Biochemicals). AP-conjugated anti-DIG antibody (1:500) was used to detect the hybridization signals (Roche Molecular Biochemicals).

Acknowledgments

REFERENCES

Abu-Issa R, Smyth G, Smoak I, Yamamura K, Meyers EN. Fgf8 is required for pharyngeal arch and cardiovascular development in the mouse. Development. 2002; 129:4613–4625. [PubMed: 12223417]

Ai D, Liu W, Ma L, Dong F, Lu MF, Wang D, Verzi MP, Cai C, Gage PJ, Evans S, Black BL, Brown NA, Martin JF. Pitx2 regulates cardiac left-right asymmetry by patterning second cardiac lineage-derived myocardium. Dev Biol. 2006; 296:437–449. [PubMed: 16836994]

Amendt BA, Sutherland LB, Semina EV, Russo AF. The molecular basis of Rieger syndrome. Analysis of Pitx2 homeodomain protein activities. J Biol Chem. 1998; 273:20066–20072. [PubMed: 9685346]

Arima Y, Miyagawa-Tomita S, Maeda K, Asai R, Seya D, Minoux M, Rijli FM, Nishiyama K, Kim KS, Uchijima Y, Ogawa H, Kurihara Y, Kurihara H. Preotic neural crest cells contribute to coronary artery smooth muscle involving endothelin signalling. Nat Commun. 2012; 3:1267. [PubMed: 23232397]

Brown CB, Boyer AS, Runyan RB, Barnett JV. Antibodies to the Type II TGFbeta receptor block cell activation and migration during atrioventricular cushion transformation in the heart. Dev Biol. 1996; 174:248–257. [PubMed: 8631497]

Buckingham M, Meilhac S, Zaffran S. Building the mammalian heart from two sources of myocardial cells. Nat Rev Genet. 2005; 6:826–835. [PubMed: 16304598]

Cai CL, Liang X, Shi Y, Chu PH, Pfaff SL, Chen J, Evans S. Isl1 identifies a cardiac progenitor population that proliferates prior to differentiation and contributes a majority of cells to the heart. Dev Cell. 2003; 5:877–889. [PubMed: 14667410]

Campbell AL, Eng D, Gross MK, Kioussi C. Prediction of gene network models in limb muscle precursors. Gene. 2012; 509:16–23. [PubMed: 22917675]

Campione M, Ros MA, Icardo JM, Piedra E, Christoffels VM, Schweickert A, Blum M, Franco D, Moorman AF. Pitx2 expression defines a left cardiac lineage of cells: evidence for atrial and ventricular molecular isomerism in the iv/iv mice. Developmental biology. 2001; 231:252–264. [PubMed: 11180966]

Dodou E, Verzi MP, Anderson JP, Xu SM, Black BL. Mef2c is a direct transcriptional target of ISL1 and GATA factors in the anterior heart field during mouse embryonic development. Development. 2004; 131:3931–3942. [PubMed: 15253934]

Echelard Y, Vassileva G, McMahon AP. Cis-acting regulatory sequences governing Wnt-1 expression in the developing mouse CNS. Development. 1994; 120:2213–2224. [PubMed: 7925022]

Eng D, Campbell A, Hilton T, Leid M, Gross MK, Kioussi C. Prediction of regulatory networks in mouse abdominal wall. Gene. 2010; 469:1–8. [PubMed: 20797427]

Eng D, Dubovoy A. High Left Ventricular Vent Return After Left and Right Ventricular Assist Device Placement in a Patient With a Mechanical Aortic Valve. J Cardiothorac Vasc Anesth. 2012

Eng D, Ma HY, Xu J, Shih HP, Gross MK, Kiouss C. Loss of abdominal muscle in Pitx2 mutants associated with altered axial specification of lateral plate mesoderm. PLoS One. 2012; 7:e42228. [PubMed: 22860089]

Engleka KA, Manderfield LJ, Brust RD, Li L, Cohen A, Dymecki SM, Epstein JA. Islet1 derivatives in the heart are of both neural crest and second heart field origin. Circ Res. 2012; 110:922–926. [PubMed: 22394517]

Franco D, Campione M. The role of Pitx2 during cardiac development. Linking left-right signaling and congenital heart diseases. Trends Cardiovasc Med. 2003; 13:157–163. [PubMed: 12732450]

Frank DU, Fotheringham LK, Brewer JA, Muglia LJ, Tristani-Firouzi M, Capecchi MR, Moon AM. An Fgf8 mouse mutant phenocopies human 22q11 deletion syndrome. Development. 2002; 129:4591–4603. [PubMed: 12223415]

Gage PJ, Rhoades W, Prucka SK, Hjalt T. Fate maps of neural crest and mesoderm in the mammalian eye. Invest Ophthalmol Vis Sci. 2005; 46:4200–4208. [PubMed: 16249499]

Gage PJ, Suh H, Camper SA. Dosage requirement of Pitx2 for development of multiple organs. Development. 1999; 126:4643–4651. [PubMed: 10498698]

Galli D, Dominguez JN, Zaffran S, Munk A, Brown NA, Buckingham ME. Atrial myocardium derives from the posterior region of the second heart field, which acquires left-right identity as Pitx2c is expressed. Development. 2008; 135:1157–1167. [PubMed: 18272591]

Ganga M, Espinoza HM, Cox CJ, Morton L, Hjalt TA, Lee Y, Amendt BA. PITX2 isoform-specific regulation of atrial natriuretic factor expression: synergism and repression with Nkx2.5. J Biol Chem. 2003; 278:22437–22445. [PubMed: 12692125]

Hamblet NS, Lijam N, Ruiz-Lozano P, Wang J, Yang Y, Luo Z, Mei L, Chien KR, Sussman DJ, Wynshaw-Boris A. Dishevelled 2 is essential for cardiac outflow tract development, somite segmentation and neural tube closure. Development. 2002; 129:5827–5838. [PubMed: 12421720]

Harel I, MY.; Avraham, R.; Rinon, A.; Ma, HY.; Cross, JW.; Leviatan, N.; Hegesh, JT.; Roy, A.; Jacob-Hirsch, J.; Rechavi, G.; Carvajal, J.; Tole, S.; Kioussi, C.; Quaggin, S.; Tzahor, E. Proceedings of the National Academy of Sciences. PNAS; 2012. Pharyngeal mesoderm regulatory network controls cardiac and head muscle morphogenesis. in press.

Harvey RP. Patterning the vertebrate heart. Nat Rev Genet. 2002; 3:544–556. [PubMed: 12094232]

Hilton T, Gross MK, Kioussi C. Pitx2-dependent occupancy by histone deacetylases is associated with T-box gene regulation in mammalian abdominal tissue. J Biol Chem. 2010; 285:11129–11142. [PubMed: 20129917]

Hoffman JI, Kaplan S. The incidence of congenital heart disease. J Am Coll Cardiol. 2002; 39:1890–1900. [PubMed: 12084585]

Hu T, Yamagishi H, Maeda J, McAnally J, Yamagishi C, Srivastava D. Tbx1 regulates fibroblast growth factors in the anterior heart field through a reinforcing autoregulatory loop involving forkhead transcription factors. Development. 2004; 131:5491–5502. [PubMed: 15469978]

Hurlstone AF, Haramis AP, Wienholds E, Begthel H, Korving J, Van Eeden F, Cuppen E, Zivkovic D, Plasterk RH, Clevers H. The Wnt/beta-catenin pathway regulates cardiac valve formation. Nature. 2003; 425:633–637. [PubMed: 14534590]

Ilagan R, Abu-Issa R, Brown D, Yang YP, Jiao K, Schwartz RJ, Klingensmith J, Meyers EN. Fgf8 is required for anterior heart field development. Development. 2006; 133:2435–2445. [PubMed: 16720880]

Joyner A, Wall N. Immunohistochemistry of whole-mount mouse embryos. CSH Protoc. 2008 2008:pdb prot4820.

Kelly RG, Brown NA, Buckingham ME. The arterial pole of the mouse heart forms from Fgf10-expressing cells in pharyngeal mesoderm. Dev Cell. 2001; 1:435–440. [PubMed: 11702954]

Kelly RG, Papaioannou VE. Visualization of outflow tract development in the absence of Tbx1 using an FgF10 enhancer trap transgene. Developmental dynamics : an official publication of the American Association of Anatomists. 2007; 236:821–828. [PubMed: 17238155]

Kioussi C, Briata P, Baek SH, Rose DW, Hamblet NS, Herman T, Ohgi KA, Lin C, Gleiberman A, Wang J, Brault V, Ruiz-Lozano P, Nguyen HD, Kemler R, Glass CK, Wynshaw-Boris A, Rosenfeld MG. Identification of a Wnt/Dvl/beta-Catenin --> Pitx2 pathway mediating cell-type-specific proliferation during development. Cell. 2002; 111:673–685. [PubMed: 12464179]

Kirby, M. Cardiac Development. New York: Oxford University Press; 2007.

Kitamura K, Miura H, Miyagawa-Tomita S, Yanazawa M, Katoh-Fukui Y, Suzuki R, Ohuchi H, Suehiro A, Motegi Y, Nakahara Y, Kondo S, Yokoyama M. Mouse Pitx2 deficiency leads to

anomalies of the ventral body wall, heart, extra- and periocular mesoderm and right pulmonary isomerism. Development. 1999; 126:5749–5758. [PubMed: 10572050]

Kyrylkova K, Kyryachenko S, Kioussi C, Leid M. Determination of gene expression patterns by in situ hybridization in sections. Methods Mol Biol. 2012; 887:23–31. [PubMed: 22566043]

Lin CR, Kioussi C, O'Connell S, Briata P, Szeto D, Liu F, Izpisua-Belmonte JC, Rosenfeld MG. Pitx2 regulates lung asymmetry, cardiac positioning and pituitary and tooth morphogenesis. Nature. 1999; 401:279–282. [PubMed: 10499586]

Lin Q, Schwarz J, Bucana C, Olson EN. Control of mouse cardiac morphogenesis and myogenesis by transcription factor MEF2C. Science. 1997; 276:1404–1407. [PubMed: 9162005]

Liu C, Liu W, Palie J, Lu MF, Brown NA, Martin JF. Pitx2c patterns anterior myocardium and aortic arch vessels and is required for local cell movement into atrioventricular cushions. Development. 2002; 129:5081–5091. [PubMed: 12397115]

Liu W, Selever J, Lu MF, Martin JF. Genetic dissection of Pitx2 in craniofacial development uncovers new functions in branchial arch morphogenesis, late aspects of tooth morphogenesis and cell migration. Development. 2003; 130:6375–6385. [PubMed: 14623826]

Liu W, Selever J, Wang D, Lu MF, Moses KA, Schwartz RJ, Martin JF. Bmp4 signaling is required for outflow-tract septation and branchial-arch artery remodeling. Proceedings of the National Academy of Sciences of the United States of America. 2004; 101:4489–4494. [PubMed: 15070745]

Lozano-Velasco E, Chinchilla A, Martinez-Fernandez S, Hernandez-Torres F, Navarro F, Lyons GE, Franco D, Aranega AE. Pitx2c modulates cardiac-specific transcription factors networks in differentiating cardiomyocytes from murine embryonic stem cells. Cells Tissues Organs. 2011; 194:349–362. [PubMed: 21389672]

Lu MF, Pressman C, Dyer R, Johnson RL, Martin JF. Function of Rieger syndrome gene in left-right asymmetry and craniofacial development. Nature. 1999; 401:276–278. [PubMed: 10499585]

Lyons KM, Pelton RW, Hogan BL. Organogenesis and pattern formation in the mouse: RNA distribution patterns suggest a role for bone morphogenetic protein-2A (BMP-2A). Development. 1990; 109:833–844. [PubMed: 2226202]

Ma L, Lu MF, Schwartz RJ, Martin JF. Bmp2 is essential for cardiac cushion epithelial-mesenchymal transition and myocardial patterning. Development. 2005; 132:5601–5611. [PubMed: 16314491]

Mao X, Fujiwara Y, Chapdelaine A, Yang H, Orkin SH. Activation of EGFP expression by Cre-mediated excision in a new ROSA26 reporter mouse strain. Blood. 2001; 97:324–326. [PubMed: 11133778]

McCulley DJ, Kang JO, Martin JF, Black BL. BMP4 is required in the anterior heart field and its derivatives for endocardial cushion remodeling, outflow tract septation, and semilunar valve development. Dev Dyn. 2008; 237:3200–3209. [PubMed: 18924235]

Monzen K, Shiojima I, Hiroi Y, Kudoh S, Oka T, Takimoto E, Hayashi D, Hosoda T, Habara-Ohkubo A, Nakaoka T, Fujita T, Yazaki Y, Komuro I. Bone morphogenetic proteins induce cardiomyocyte differentiation through the mitogen-activated protein kinase kinase kinase TAK1 and cardiac transcription factors Csx/Nkx-2.5 and GATA-4. Mol Cell Biol. 1999; 19:7096–7105. [PubMed: 10490646]

Niessen K, Karsan A. Notch signaling in cardiac development. Circ Res. 2008; 102:1169–1181. [PubMed: 18497317]

Nowotschin S, Liao J, Gage PJ, Epstein JA, Campione M, Morrow BE. Tbx1 affects asymmetric cardiac morphogenesis by regulating Pitx2 in the secondary heart field. Development. 2006; 133:1565–1573. [PubMed: 16556915]

Oliver G, Wehr R, Jenkins NA, Copeland NG, Cheyette BN, Hartenstein V, Zipursky SL, Gruss P. Homeobox genes and connective tissue patterning. Development. 1995; 121:693–705. [PubMed: 7720577]

Park EJ, Watanabe Y, Smyth G, Miyagawa-Tomita S, Meyers E, Klingensmith J, Camenisch T, Buckingham M, Moon AM. An FGF autocrine loop initiated in second heart field mesoderm regulates morphogenesis at the arterial pole of the heart. Development. 2008; 135:3599–3610. [PubMed: 18832392]

Perveen R, Lloyd IC, Clayton-Smith J, Churchill A, van Heyningen V, Hanson I, Taylor D, McKeown C, Super M, Kerr B, Winter R, Black GC. Phenotypic variability and asymmetry of Rieger syndrome associated with PITX2 mutations. Invest Ophthalmol Vis Sci. 2000; 41:2456–2460. [PubMed: 10937553]

Ray HJ, Niswander L. Mechanisms of tissue fusion during development. Development. 2012; 139:1701–1711. [PubMed: 22510983]

Romano LA, Runyan RB. Slug is an essential target of TGFbeta2 signaling in the developing chicken heart. Dev Biol. 2000; 223:91–102. [PubMed: 10864463]

Schnabel RB. Comparison of approaches to fine-map first-generation genome-wide association study results at chromosome 9p21. Circ Cardiovasc Genet. 2011; 4:577–578. [PubMed: 22010166]

Shih HP, Gross MK, Kioussi C. Cranial muscle defects of Pitx2 mutants result from specification defects in the first branchial arch. Proceedings of the National Academy of Sciences of the United States of America. 2007a; 104:5907–5912. [PubMed: 17384148]

Shih HP, Gross MK, Kioussi C. Expression pattern of the homeodomain transcription factor Pitx2 during muscle development. Gene Expr Patterns. 2007b; 7:441–451. [PubMed: 17166778]

Tessari A, Pietrobon M, Notte A, Cifelli G, Gage PJ, Schneider MD, Lembo G, Campione M. Myocardial Pitx2 differentially regulates the left atrial identity and ventricular asymmetric remodeling programs. Circ Res. 2008; 102:813–822. [PubMed: 18292603]

Tirosh-Finkel L, Elhanany H, Rinon A, Tzahor E. Mesoderm progenitor cells of common origin contribute to the head musculature and the cardiac outflow tract. Development. 2006; 133:1943–1953. [PubMed: 16624859]

Verzi MP, McCulley DJ, De Val S, Dodou E, Black BL. The right ventricle, outflow tract, and ventricular septum comprise a restricted expression domain within the secondary/anterior heart field. Dev Biol. 2005; 287:134–145. [PubMed: 16188249]

Vitelli F, Morishima M, Taddei I, Lindsay EA, Baldini A. Tbx1 mutation causes multiple cardiovascular defects and disrupts neural crest and cranial nerve migratory pathways. Human molecular genetics. 2002; 11:915–922. [PubMed: 11971873]

Waldo K, Miyagawa-Tomita S, Kumiski D, Kirby ML. Cardiac neural crest cells provide new insight into septation of the cardiac outflow tract: aortic sac to ventricular septal closure. Dev Biol. 1998; 196:129–144. [PubMed: 9576827]

Waldo KL, Hutson MR, Stadt HA, Zdanowicz M, Zdanowicz J, Kirby ML. Cardiac neural crest is necessary for normal addition of the myocardium to the arterial pole from the secondary heart field. Dev Biol. 2005; 281:66–77. [PubMed: 15848389]

Waldo KL, Lo CW, Kirby ML. Connexin 43 expression reflects neural crest patterns during cardiovascular development. Dev Biol. 1999; 208:307–323. [PubMed: 10191047]

Webb S, Qayyum SR, Anderson RH, Lamers WH, Richardson MK. Septation and separation within the outflow tract of the developing heart. J Anat. 2003; 202:327–342. [PubMed: 12739611]

Xu H, Morishima M, Wylie JN, Schwartz RJ, Bruneau BG, Lindsay EA, Baldini A. Tbx1 has a dual role in the morphogenesis of the cardiac outflow tract. Development. 2004; 131:3217–3227. [PubMed: 15175244]

Yashiro K, Shiratori H, Hamada H. Haemodynamics determined by a genetic programme govern asymmetric development of the aortic arch. Nature. 2007; 450:285–288. [PubMed: 17994097]

Zhou W, Lin L, Majumdar A, Li X, Zhang X, Liu W, Etheridge L, Shi Y, Martin J, Van de Ven W, Kaartinen V, Wynshaw-Boris A, McMahon AP, Rosenfeld MG, Evans SM. Modulation of morphogenesis by noncanonical Wnt signaling requires ATF/CREB family-mediated transcriptional activation of TGFbeta2. Nat Genet. 2007; 39:1225–1234. [PubMed: 17767158]

- Pitx2 controls cellularity of conotruncus.

- Pitx2 regulates inductive signaling for endocardial cushion formation.

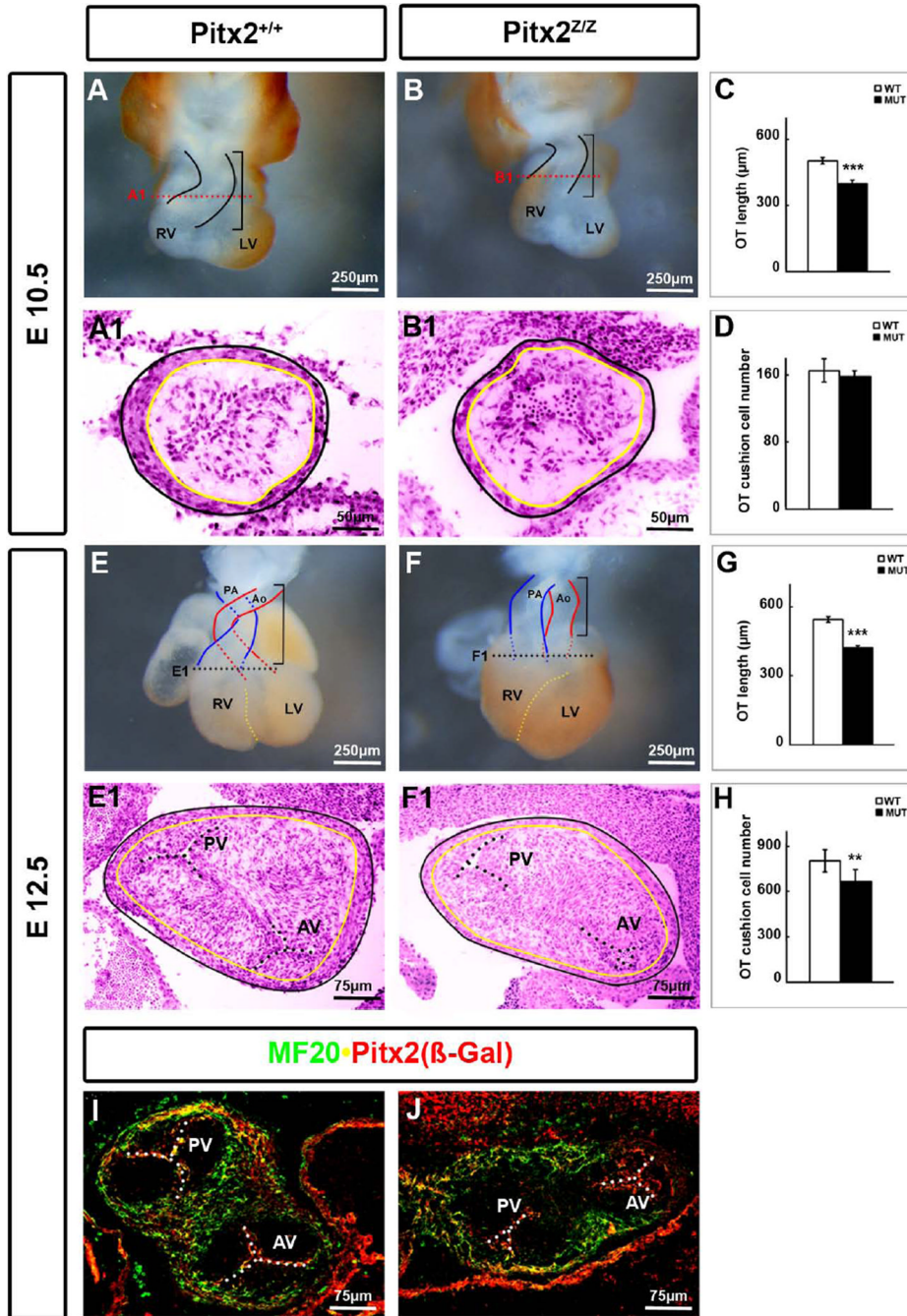- Pitx2 is a node of the network kernel for OT development.

Figure 1. Shorter and Hypocellular Cardiac OT in *Pitx2* Mutants
Ventral view of the entire heart at E10.5 **(A, B)** and E12.5 **(E, F)** showed a shortened OT with a prominent DORV in *Pitx2*-mutant mice **(F)**. **(C, G)** The length of the OT was measured as indicated by brackets. Statistics were based on results from 3 different embryos at each stage. HE staining on 14 μm transverse cryosections at E10.5 **(A1, B1)** and E 12.5 **(E1, F1)** mice indicated thinner OT epithelium in the conus. The black and yellow lines correspond to the outer and inner epithelium, respectively. **(D, H)** Cell counts of a set of 5–8 serial sections along the OT showed reduction of cells in the cushions of mutants. ***: $p<0.01$, **: $p<0.05$. **(I, J)** Double labeling immunohistochemistry on E12.5 mouse

transverse sections for MF20 and Pitx2 (β-Gal). No MF20^{+} cells were detected in the conal septum and semilunar valves in the mutants. Ao, aorta; AV, aortic valve; LV, left ventricle; PA, pulmonary artery; PV, pulmonary valve; RV, right ventricle.
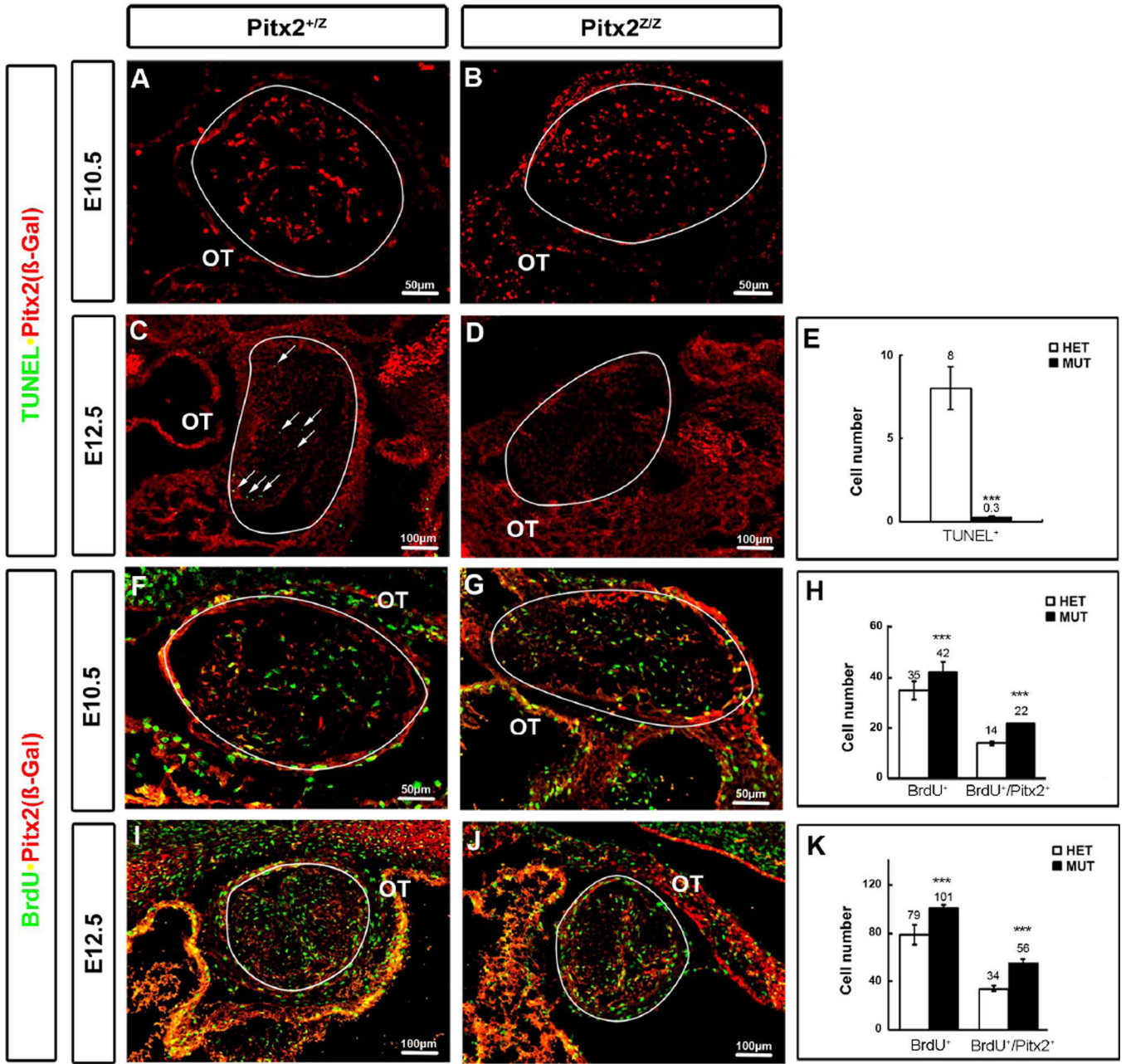
Figure 2. OT Cushion Mesenchymal Cell Proliferation and Apoptosis Defects in *Pitx2* Mutants
TUNEL assay **(A–D)** was performed on 14 μm frontal sections to identify the cell apoptosis index during OT remodeling. TUNEL signal was not detected at E10.5 in either OT mesenchyme of the heterozygote or in mutant littermates **(A, B)**. The TUNEL signal was detected in heterozygote OT cushion mesenchyme (**C,** white arrows) but not in mutant littermate **(D)** at E12.5. The number of apoptotic cells in the OT cushion was counted based on eight continuous sections for three individual embryos at E12.5 **(E)**. Double labeling of β-gal and Bromodeoxyuridine (BrdU) on 14 μm frontal sections showed Pitx2 effects on cell proliferation **(F, G, I, J)**. The number of proliferative cells was increased in *Pitx2* mutants at E10.5 and E12.5, respectively **(H, K)**. The BrdU$^+$ and BrdU$^+$/Pitx2$^+$ cells were counted based on five continuous sections for three individual embryos in each stage. The OT

cushion was traced by a white line. Statistics were based on results from 3 different embryos at each stage. ***: p<0.01.
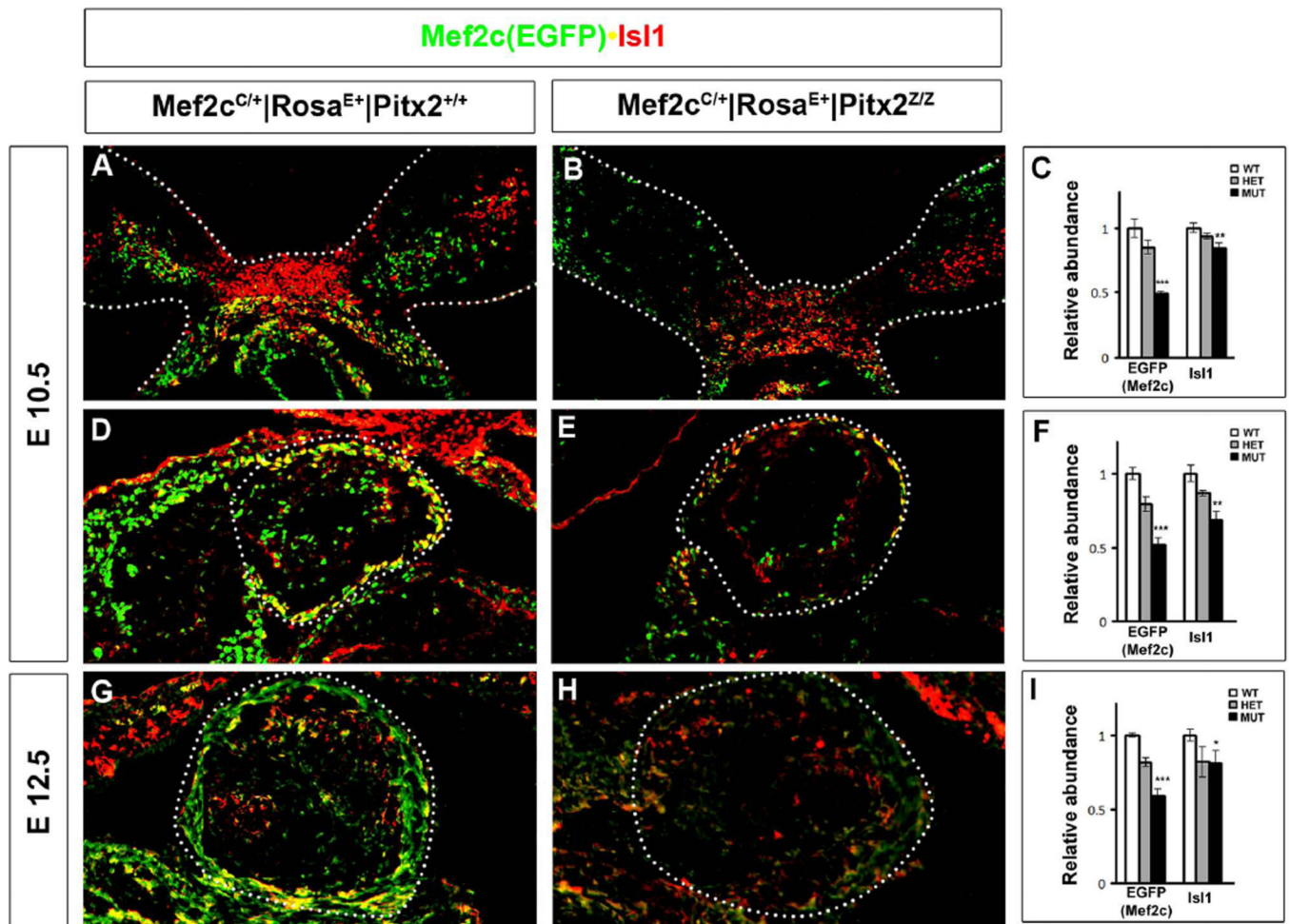
Figure 3. Defects of the Second Cardiac Cell Lineage in *Pitx2* Mutants
Double labeling immunohistochemistry of transverse cryosections sections of $Mef2c^{Cre/+}|$
$Rosa^{EGFP/+}|Pitx2^{+/+}$ **(A, D, G)** and $Mef2c^{Cre/+}|Rosa^{EGFP/+}|Pitx2^{Z/Z}$ **(B, E, H)** for EGFP
(Mef2c) and Isl1 indicated reduction of cell populations in the mutant BA **(B)** at E10.5 and
OT at E10.5 **(E)** and E12.5 **(H). (G, F, I)** Quantitative analysis by qPCR for *EGFP* and *Isl1*
indicated reduced levels in E10.5 BA **(C)** and OT **(F, I)**. ***: $p<0.01$; **: $p<0.05$; *: $p<0.1$.
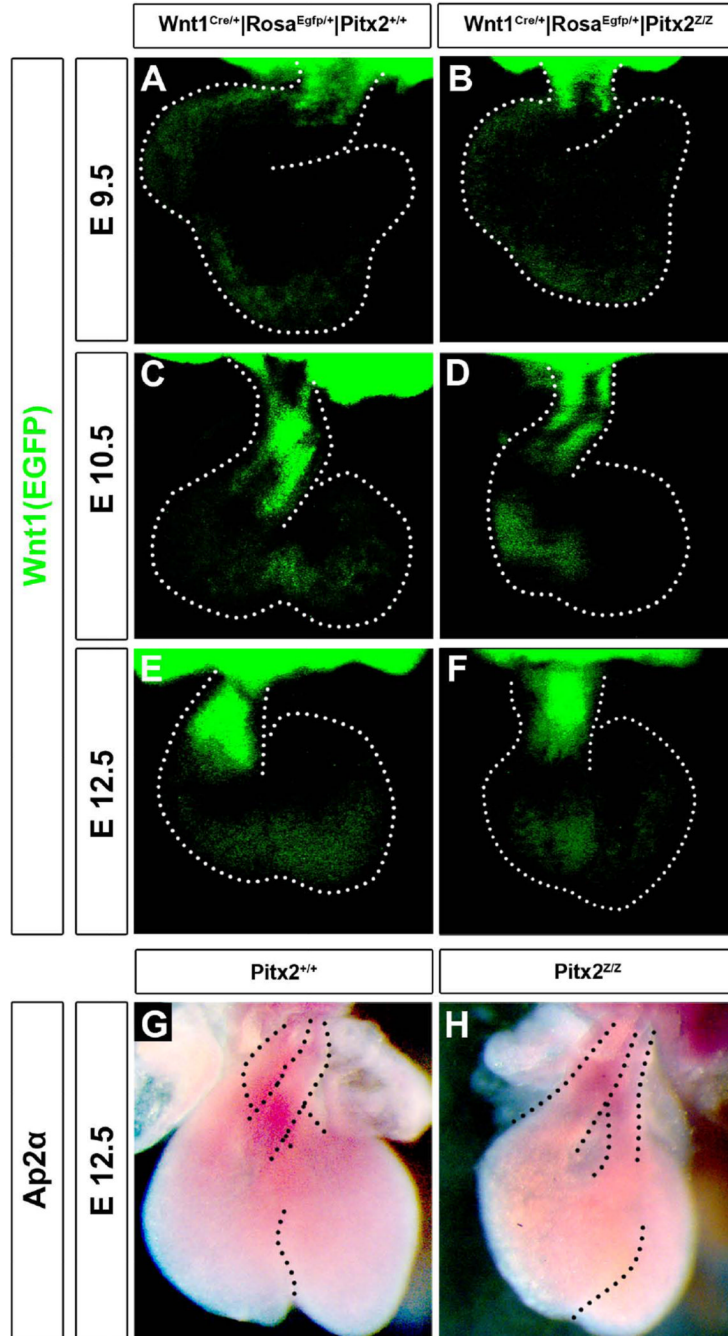
Figure 4. Impaired cNC cells in *Pitx2* mutants

*Wnt1^Cre/+^|Rosa^EGFP^|Pitx2^+/+^* (**A, C, E**) and *Wnt1^Cre/+^|Rosa^EGFP^|Pitx2^Z/Z^* (**B, D, F**) hearts were dissected at E 9.5 (**A, B**), E 10.5 (**C, D**) and E 12.5 (**E, F**). The green fluorescent cNC cells that migrated towards the OT were reduced in mutants, with more prominent phenotype at E9.5 and E10.5. (**G, H**) Whole mount RNA in situ hybridization at E12.5 hearts for *Ap2α* expression indicated reduced levels in the great arteries in mutants.
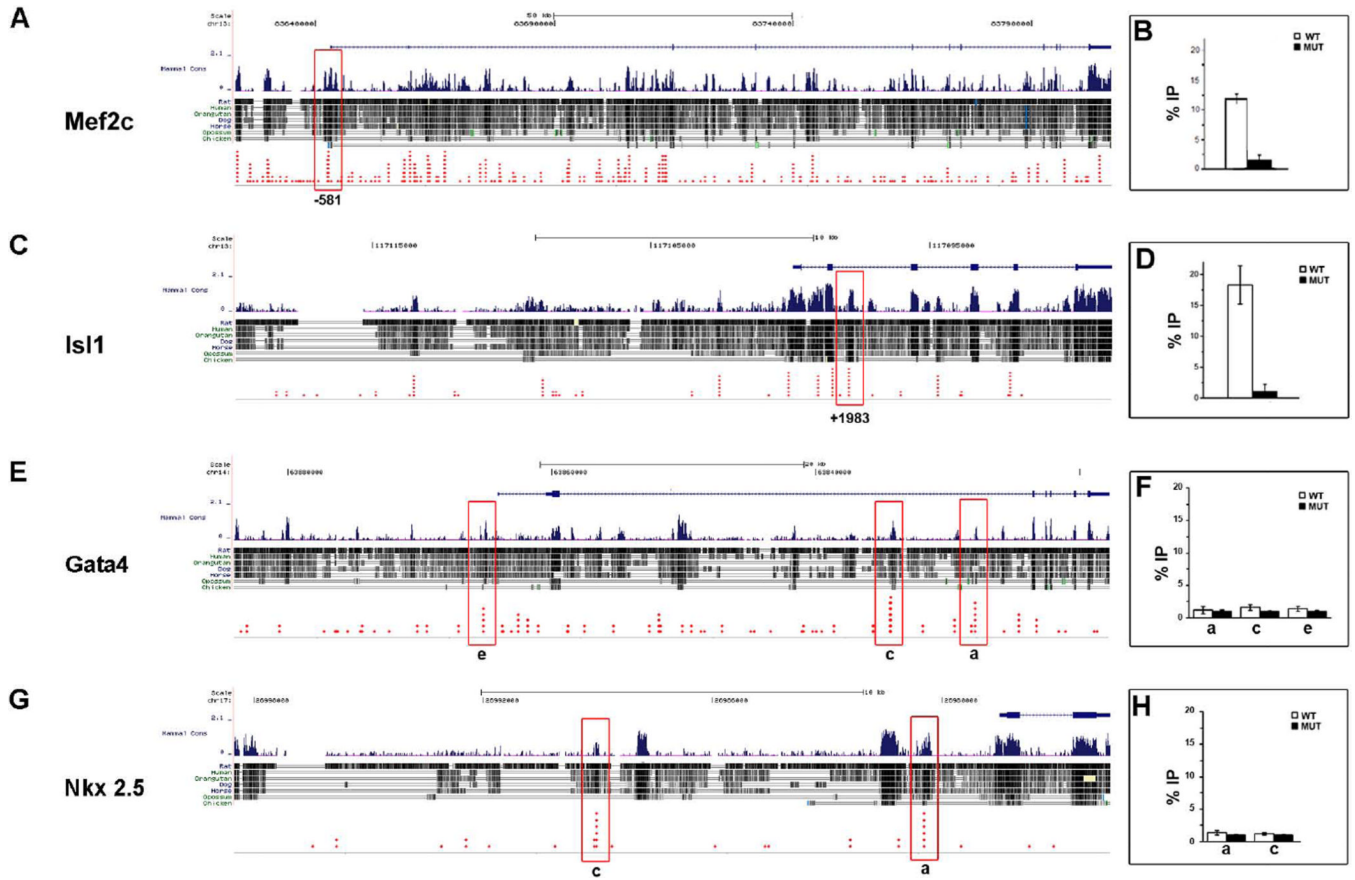
Figure 5. Pitx2 Occupancy on SSTF Gene Loci in BA and Heart Chromatin
Sonically sheared chromatin, isolated from E10.5 mice, was used to detect Pitx2 protein occupancy on *Mef2c* (**A**) and *Isl1* (**B**) in BA biopsies and *Gata4* (**E**) and *Nkx2.5* (**G**) in heart biopsies. PCR amplicons of 70–150bp (red boxes) were designed around highly evolutionarily conserved bicoid core motif TAATCY. Each red diamond indicated a single vertebrate species, containing the biocoid core motif. Bar graphs show the average relative amount of signal precipitated from wild type (white bar) and mutant (black bar). Pitx2 was found to occupy the *Mef2c* and *Isl1* gene on the conserved −521 (**B**) and +1983 (**D**) sites in E10.5 embryonic BA biopsies, respectively. No significant difference was measured for Pitx2 occupancy in conserved regions of Gata4 (**F**) and Nkx2.5 (**H**) in E10.5 heart biopsies.

Figure 6. Alteration of FGF, BMP and Notch Signaling in *Pitx2* Mutants
RNA in situ hybridization on cryostat sections revealed altered *Fgf8* (**A–C**), *Fgf3* (**E–G**), *Notch2* (**I–K**) and *Bmp4* (**M–O**) expression in E10.5 *Pitx2* control (wild type and heterozygote) and mutant mice. The *Fgf8* expression in 3rd and 4th BA ectoderm was decreased in mutants compared to control embryos (**C**). *Fgf3* expression levels were reduced in the 2nd – 6th BA mutants (**G**). *Notch2* expression levels, detected in the 3rd and 4th BA in wild type (**I**) and heterozygote (**J**), were barely detectable in 3rd and 4th BA in mutants (**K**). No *Bmp4* expression was detected in the OT mesenchymal cushions (area inside the black dotted line) in mutants (**O**) compare to the control (**M, N**). Thinner OT wall (between red and black dotted line) was consistently observed in Pitx2 mutants (**O**). Quantitative PCR assay indicated the significantly decreased mRNA expression levels of *Fgf8* (**D**), *Fgf3* (**H**), *Notch2* (**L**) and *Bmp4* (**P**) at E10.5 BA (D, H, L) and heart (**P**) biopsies, respectively.
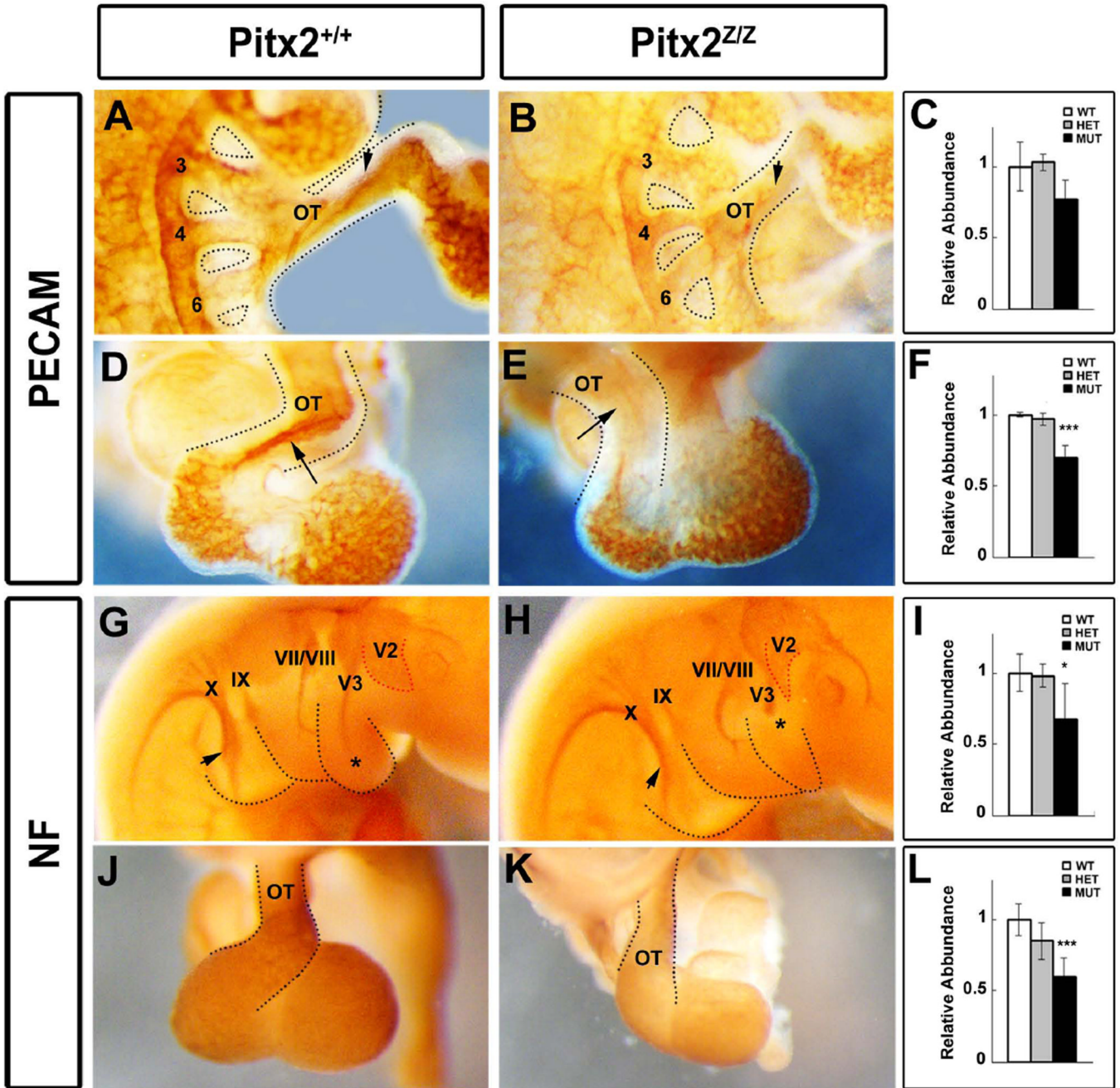
Figure 7. Vascular and Nervous System Defects in *Pitx2* Mutants

Whole mount antibody staining with PECAM **(A, B, D, E)** and NF **(G, H, J, K)** was performed on E10.5 *Pitx2* wild type and mutant mice. PECAM expression is reduced in BA (3, 4 and 6) and OT **(A, B**, arrowhead). The dorsal view of the OT **(D, E)** indicated the septational vasculature (arrow) was disrupted in Pitx2-null mice. **(C, F)** Quantitative qPCR for PECAM mRNA levels in *Pitx2* wild type, heterozygote and mutant in BAs **(C)** and heart **(F)** biopsies. The expression levels of PECAM in heart were significantly decreased in E10.5 mutants. Innervation of BAs and OT was detected by NF antibody in both control and mutant embryos **(G, H, J, K)**. V2 (red dotted line) and V3 (stars) and X (arrow head) were shorter and thinner in mutants **(H)**. NF signals were reduced in mutant hearts **(K)**.

Quantitative qPCR assay indicated significantly decreased levels in mutants in BA **(I)** and OT **(L)** biopsies, with no difference between wild type and heterozygote at this stage. V2: maxillary nerve; V3: Mandibular nerve; VII/VIII: Facial nerve; IX: Glossopharyngeal nerve; X: Vagus nerve.

Table 1

qPCR primer sets

Primer	Forward	Reverse
qPCR		
EGFP	ACGTAAACGGCCACAAGTTC	AAGTCGTGCTGCTTCATGTG
Isl1	ATGATGGTGGTTTACAGGCTAAC	TCGATGCTACTTCACTGCCAG
Fgf8	CCGAGGAGGGATCTAAGGAAC	CTTCCAAAAGTATCGGTCTCCAC
Fgf3	TGCGCTACCAAGTACCACC	CACTTCCACCGCAGTAATCTC
Notch2	ATGTGGACGAGTGTCTGTTGC	GGAAGCATAGGCACAGTCATC
Bmp4	TTCCTGGTAACCGAATGCTGA	CCTGAATCTCGGCGACTTTTT
PECAM	ACGCTGGTGCTCTATGCAAG	TCAGTTGCTGCCCATTCATCA
NF	ACAGCTCGGCTATGCTCAG	CGGGACAGTTTGTAGTCGCC
GAPDH	AGGTCGGTGTGAACGGATTTG	TGTAGACCATGTAGTTGAGGTCA
ChIP-qPCR		
Isl1	TTGGGGTGACTCTTCCTTTG	GATGGGCAATTTGATCTGCT
Mef2c	CCATGACCATCCAGTTTTGA	GCACACACTTGCTTCATTTCA
Nkx2.5a	GGGCGAGGGTCCTGGGAGTC	CGGCCCCCAATATAGCTCCCC
Nkx2.5c	ACTGACACACACTGCAGGGGC	GTGGGTGGTCCTCTCTCAGCAGT
Gata4a	TGTCCAACAATGGCTGTGGAGTGC	TCCCTAGTTCCTCTGTCCCTTGCC
Gata4c	AAGCCCCCATCCCCTGCACTT	ACTGGACAGAACCTTGCCTGCTCA
Gata4e	TTCTCTCCCCGGCACCGGTTT	GTCCTCGAACTGCGGGAGCC